

Effect of lung inhomogeneity on dose distribution during radiotherapy of patient with lung cancer

M. Zabihzadeh^{1,2,3*}, Z. Ghahremani², S.M. Hoseini³, H. Shahbazian³,
M. Hoseini Ghahfarokhi⁴

¹Cancer Research Center, Ahvaz Jundishapur University of Medical Sciences, Ahvaz, Iran

²Department of Medical Physics, School of Medicine, Ahvaz Jundishapur University of Medical Sciences, Ahvaz, Iran

³Department of Clinical Oncology, Golestan Hospital, Ahvaz Jundishapur University of Medical Sciences, Ahvaz, Iran

⁴Radiology and Nuclear Medicine, Kermanshah University of Medical Sciences, Kermanshah, Iran

ABSTRACT

Background: Presence of inhomogeneities such as lung tissue with low density can perturb the dose distribution in the path of therapeutic photon beam and causes undesired cold or hot spots. The aim of this study was to investigate the effect of lung tissue inhomogeneities on dose distribution in thorax irradiation. **Materials and Methods:** The Monte Carlo simulation (MC) code of EGSnrc-based BEAMnrc was used to calculate dose distribution for 6 MV- Siemens Primus linear accelerator (Linac) in a homogenous phantom. Dose perturbation and inhomogeneity corrected factors (ICFs) were calculated due to implementation of lung tissue depended to the lung density and field size. **Results:** The maximum increased dose in lung tissue with lung density of 0.5 and 0.25gr/cm³ was 15.9%, 16.2%, 15.6%, 23.8 %, 24.8% and 25.0% for 6 × 6, 10 × 10 and 20 × 20 cm² field sizes, respectively. The maximum ICF for these field sizes was 1.16 and 1.25 for lung density of 0.5 and 0.25gr/cm³, respectively. The maximum dose reduction in lung tissue with density of 0.25 and 0.5gr/cm³ was 19.5% and 4.2 %, and the related ICF was estimated 0.84 and 0.95, respectively. **Conclusion:** Involvement of lung tissue in the path of irradiation perturbs the dose distribution which is dependent to the lung density and field size. The ICFs resulted from our MC model could be useful to accurately calculate the dose distribution in radiotherapy of lung abnormalities.

Keywords: Electronic disequilibrium, lung cancer radiotherapy, Monte Carlo simulation, inhomogeneity correction factor.

► Original article

*Corresponding authors:

Mansour Zabihzadeh, Ph.D.,

E-mail:

manzabih@gmail.com

Revised: July 2019

Accepted: August 2019

Int. J. Radiat. Res., July 2020;
18(3): 579-586

DOI: 10.18869/acadpub.ijrr.18.3.579

INTRODUCTION

Lung cancer is the leading cause of cancer-induced death among both men and women in the U.S., responsible for 161,840 deaths in 2008. Only 15% of those diagnosed with lung cancer survive for five years after diagnosis ⁽¹⁾. Radiotherapy with megavoltage photon beam is one of the major options to treat the lung cancer beside the surgery and chemotherapy strategy. Accurate delivery of the prescribed maximum dose to the tumour volume with minimum dose

to the peripheral healthy tissues has been still remained as a main challenge in radiation treatment, so that the necessary accuracy may be required to be within 2–3% ⁽²⁾.

Dose calculation by many algorithms in the presence of large inhomogeneities such as lung tissue is challenging due to lack of charge particle equilibrium; as well wide range of lung density throughout the patient's breathing cycle ⁽³⁻⁵⁾. Mesbahi *et al.* (2014) investigated the effect of electronic disequilibrium on lung dose with small photon beams. They showed that the dose

reduction with small fields in the lung was very enormous and this inaccurate prediction of absorbed dose inside lung and also lung soft-tissue interfaces may lead to critical consequences for treatment outcome ⁽⁶⁾. Furthermore, movement of lung tissue during inspiration is crucial to gating and tumour tracking ⁽⁷⁾. Chang-li *et al.* (2015) evaluated the impact of respiratory motion on dose distribution of 3DCRT (three-dimensional conformal radiotherapy) and IMRT (intensity-modulated radiotherapy). They resulted that the respiratory motion could blur the target dose distribution of 3DCRT and IMRT; the respiratory motion largely affected the marginal dose distribution of 3D-CRT, while affected the whole target volumes of IMRT ⁽⁸⁾.

Owing to these challenges accurate dose measurements by dosimeters or dose calculations by treatment planning systems (TPSs) are limited under conditions of realistic composition and geometry. The dosimetric errors during treatment of lung tumors with stereotactic body radiation therapy were studied by Altunbas *et al.* (2013). Their results indicate that dosimetric bias introduced by unit tissue density plans cannot be characterized as underestimation or overestimation of dose without taking the tumor location into account ⁽⁹⁾. Senthilkumar and Ramakrishnan (2011) develop a low cost homogeneous and heterogeneous phantom and compared the measured absorbed dose by ionization chamber with the values of 3-D Plato TPS for different radiotherapy treatment techniques. Their results confirmed that Heterogeneity correction would definitely improve the cancer treatment of the heterogeneity region ⁽¹⁰⁾.

To estimate the dose perturbations due to the heterogeneities, Monte Carlo (MC) calculation has been proved to be a useful tool, because it adequately accounts for the lack of electron equilibrium close to the different interfaces by considering the density effect when simulate the photon and electron transport within the patient body ^(6, 11).

In this study dose perturbation in presence of different densities of lung tissues was

calculated by EGSnrc-based MC code; BEAMnrc and DOSXYZnrc and the purpose was to calculate the essential inhomogeneity correction factors (ICFs) in different depths upper or lower from the lung inhomogeneities. The calculated Quantitative data in this study could be used as guideline to help physicists to evaluate and/or correct the dose distribution estimated manually or produced by different TPS algorithms in present of lung inhomogeneity across the beamline.

MATERIALS AND METHODS

Measurements

The PPDs and dose profiles (at depth of 10 cm) of 6 MV Linac (Siemens Primus, Germany) were measured by 0.13 cm³ ionization chamber (PTW, Freiburg, Germany) with DOSE1 electrometer (Scanditronix-Wellhofer, Germany) for field size of 6 × 6, 10 × 10 and 20 × 20 cm². All dose measurements were carried out at source to surface distance (SSD) of 100 cm in a IBA-Blue water phantom (IBA dosimetry Schwarzenbruck, Germany) with dimensions of 50 cm³ and were processed by dosimetry software of RFaPlus (Version 5.2, Scanditronix-Wellhofer, Germany). Each measurement was repeated three times with precision of ± 0.2%. The recommendations of international atomic energy agency (IAEA) protocol, TRS-398 ⁽¹²⁾ were followed during dose measurements.

MC calculation

The Linac head (Siemens Primus-6 MV photon mode, Germany) was modelled by EGSnrc-based BEAMnrc code ⁽¹³⁾ as described in our previous work. All needed dimensions and materials to build the MC model of Linac head were extracted from vendor data. Using the BEAMnrc code the exit window, target, primary collimator and flattening filter, monitoring chambers, mirror and jaws were simulated by proper component modules (CMs) including of SLAB, FLATFILT, CHAMBER, MIRROR and JAWS, respectively. The components of modelled Linac head are shown in figure 1.

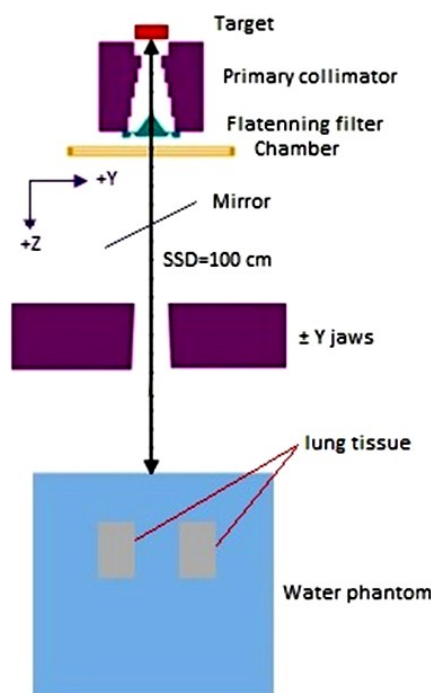


Figure 1. Schematic view of simulated 6 MV- Siemens Primus Linac head and a lung tissue contained phantom for dose calculation.

Different parameters of incident electron beam (such as energy and radial distribution) were tuned by trial and error method until to reach an ideal matching between measured and calculated PPDs and dose profile curves. The phase space file for each field size was generated at the source-to-surface distance (SSD) of 100 cm. The number of histories was dependent on the field size, e.g. 100×10^6 , 50×10^6 and 20×10^6 particles for 6×6 , 10×10 and 20×20 cm² field sizes, respectively. The DOSXYZnrc code was used to calculate the dose in defined voxels of water phantom with dimensions of 50 cm³. The voxel size was set to $1 \times 1 \times 0.2$ and $0.2 \times 1 \times 1$ cm³ to calculate the PDD and cross-line dose profile curves, respectively. The homogenous soft tissue and inhomogeneous lung tissue phantoms were simulated separately. The components of soft tissue ($\rho=1$ gr/cm³) and lung tissue ($\rho=0.25$ and 0.5 gr/cm³) were obtained from ICRU, report No. 44 ⁽¹⁴⁾. For inhomogeneous phantom, the dimension of each two lung tissues was $6 \times 15 \times 10$ cm³ and located in depth of 4 cm from the surface of soft tissue phantom. Irradiation of phantoms were

modelled for two anterior-posterior (AP) and lateral (LAT) irradiation projections.

The dose difference percentage (%D_{Difference}) was calculated using the equation 1 at a given depth:

$$\%D_{Difference} = \frac{D_{Soft\ tissue} - D_{Lung\ tissue}}{D_{Soft\ tissue}} \times 100 \quad (1)$$

Where $D_{soft\ tissue}$ is a dose at a depth in the homogeneous soft tissue phantom and $D_{lung\ tissue}$ is the dose at same depth in the inhomogeneous lung phantom.

The inhomogeneity correction factor (ICF) from the equation 2 is the ratio of dose at a depth in the inhomogeneous lung phantom ($D_{lung\ tissue}$) to the dose at same depth in the homogeneous soft tissue phantom ($D_{soft\ tissue}$).

$$ICF = \frac{D_{Lung\ tissue}}{D_{Soft\ tissue}} \quad (2)$$

All calculations were executed until the maximum statistical uncertainty of each detector reached $< \%0.5$ inside the field and $< \%1$ outside the field. To assess this statistical uncertainty, the history number of 4×10^9 was sampled from the loaded phase space file. The variance reduction method of directional Bremsstrahlung splitting (DBS) technique with splitting number of 1000 was used. In all calculations, ECUT, AE, PCUT and AP were set to 0.700 and 0.01 MeV, respectively. The electron range reduction method with ESAVE_GLOBAL= 2 MeV was defined in all designed CMs of linac head exception for the CM of target where ESAVE_GLOBAL was 0.700 MeV. All other parameters were set to default values. All runs were performed on a machine with 21×3.00 GHz CPU and 16 GB of RAM by parallel processing.

RESULTS

Validation of MC 6 MV siemens linac head

In this study, the MC simulation was applied for obtaining PDD in homogeneous and inhomogeneous lung phantom. The mean energy of 6.2 MeV, the Gaussian energy spread with

FWHM=1 MeV and the Gaussian spatial spread with FWHM=1 mm for incident electron beam were used to gain the best agreement between the measurements and MC calculations. The maximum relative error was < 1% for dose profile. The measured and calculated PDD and dose profile curves are shown in figure 2. The estimated gamma index (<1) shows that the MC calculated and measured PDDs and dose profiles are in good agreement for all investigated fields. The MC relative errors were < 0.5% for PDD curves, except for the first build up voxel that

was not reported here where the measurements could be affected by the inherent volume of the ion chamber ⁽¹⁵⁾ and also by electron contaminations ⁽¹⁶⁾. The maximum relative error was <1 % for dose profile near the field edges. These accuracies were less than the recommended value of 2% ⁽¹⁷⁾. The source of these negligible differences may be potentially originated from inaccurate provided data by the vendor or/and non-ideal tuning of incident electron beam parameters due to its time consuming process.

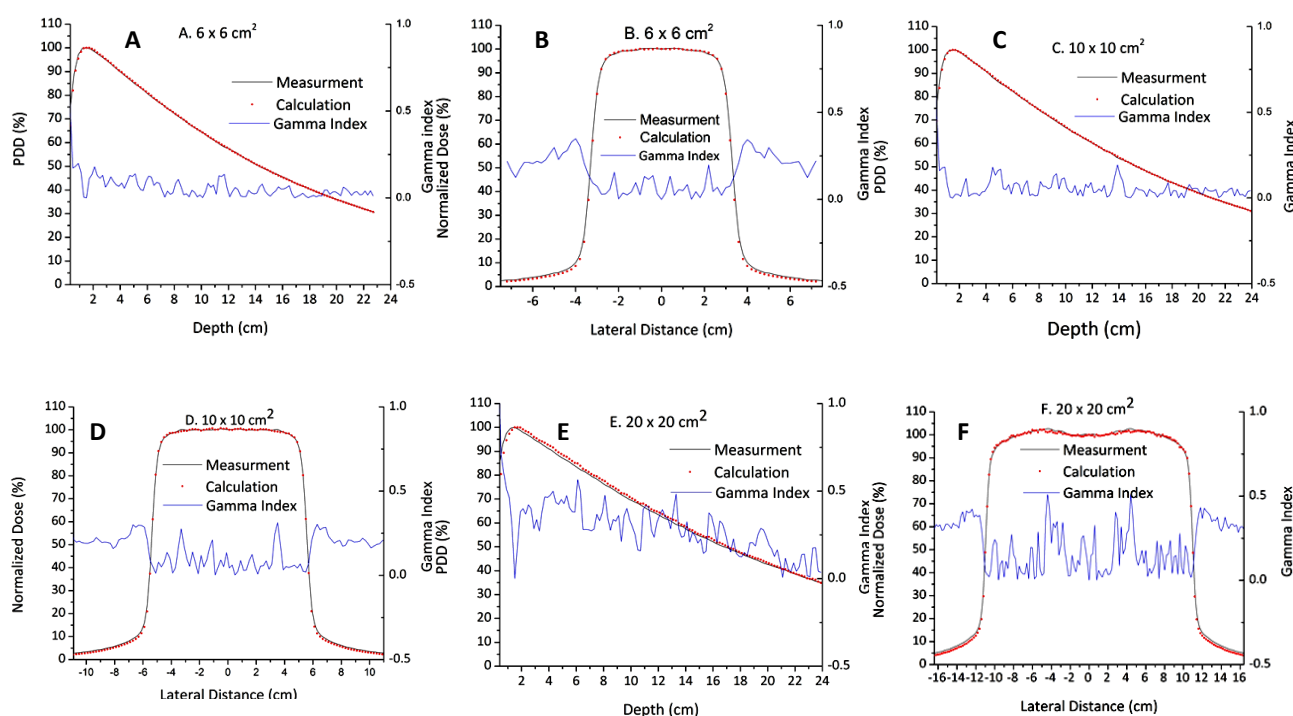
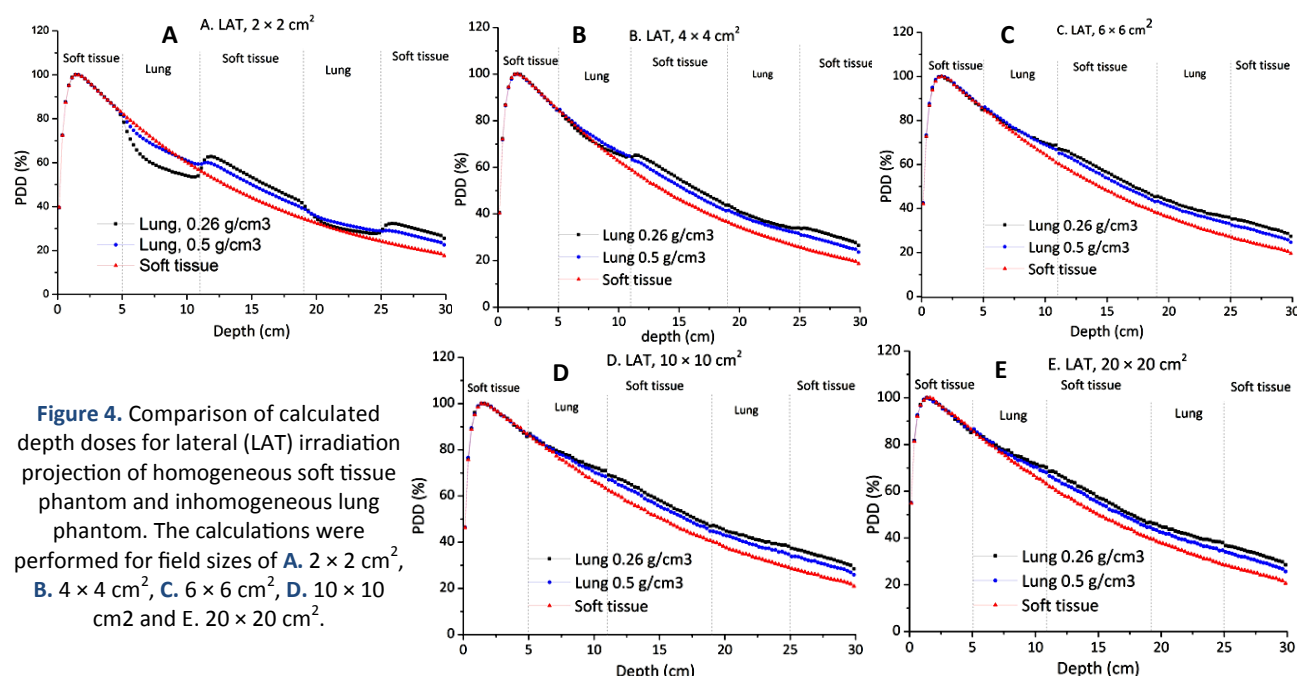
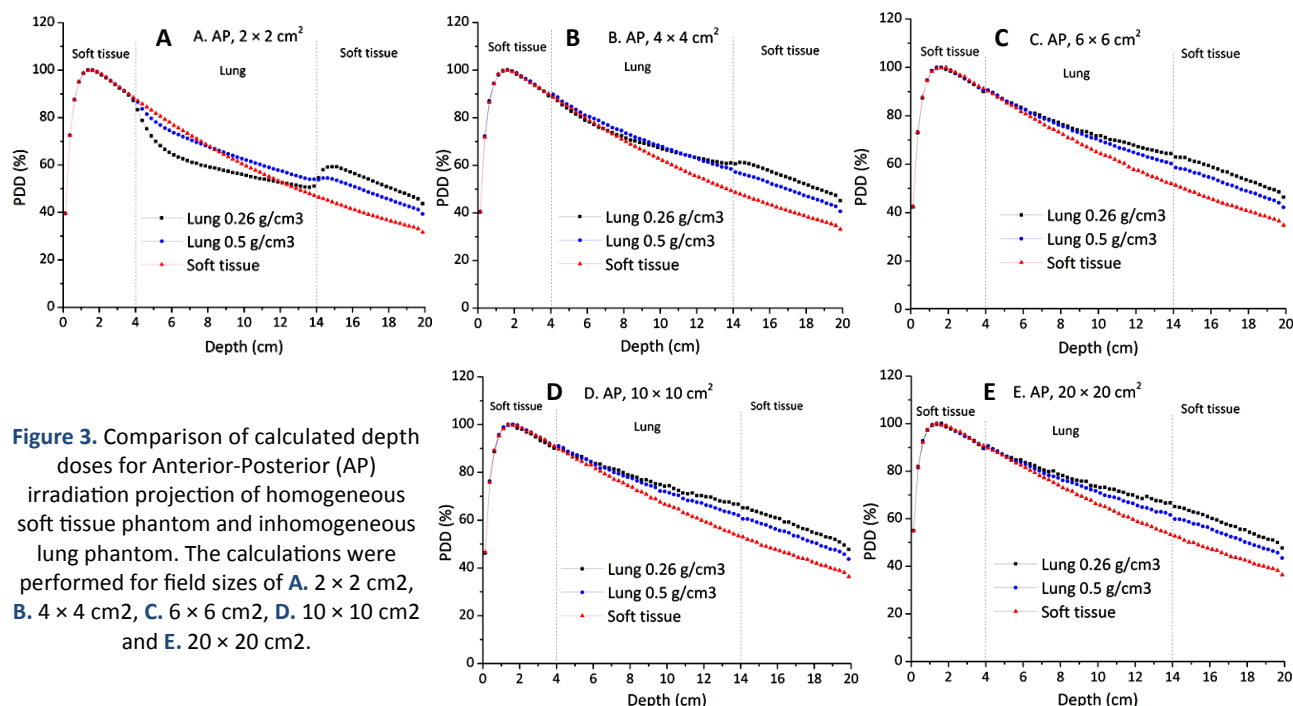


Figure 2. Comparison of calculated depth dose and dose profile curves with measurements for homogeneous water phantom to benchmark the MC model. The calculated and measured PDD for field size of **A.** $6 \times 6 \text{ cm}^2$, **C.** 10×10 and **E.** $20 \times 20 \text{ cm}^2$. The calculated and measured dose profile curve for field size of **B.** $6 \times 6 \text{ cm}^2$, **D.** 10×10 and **F.** $20 \times 20 \text{ cm}^2$. The estimated gamma index (<1) shows that the MC calculated and measured data are in good agreement.

MC calculated dose in homogenous soft tissue and inhomogeneous lung phantom

In this study, the PDD curves in homogenous soft tissue and inhomogeneous lung phantom were calculated and compared for field sizes of 2×2 , 4×4 , 6×6 , 10×10 and $20 \times 20 \text{ cm}^2$ for AP (figure 3) and LAT (figure 4) directions. For large field sizes, less attenuation of primary

photon is predominate in absorbed dose and as expected dose in the lung region is higher compared to same depths in homogeneous soft tissue; i.e. 15.9%, 16.2% and 15.6% at the end edge of lung-soft tissue interface with lung density of 0.5 gr/cm^3 for 6×6 , 10×10 and $20 \times 20 \text{ cm}^2$ field sizes, respectively.



DISCUSSION

The effect of soft tissue-lung interface on dose is apparent from figures 3 and 4. Perturbation of dose in presence of lung inhomogeneity compared to homogeneous soft tissue is highly depended to field sizes, depths

and lung density. Less attenuation of primary photons when photon entering to lung tissue increase dose to the lung. However, at the same time, lower number of scattered photons in lung compared to soft tissue reduce lung dose. Decrease the lung density increase the overestimated dose at all depths beyond the first

soft tissue-lung interface, i.e. 23.8 %, 24.8% and 25.0% for lung density of 0.25gr/cm³. Hence, maximum calculated ICFs at the end edge of lung region for these large fields are greater than unit and reach to maximum of 1.16 and 1.25 for lung density of 0.5 and 0.25gr/cm³, respectively. Mesbahi *et al.* (2006) ⁽¹⁸⁾ evaluated the Eclipse TPS for lung dose calculations for 8 and 15MV photon beams of Varian 21EX linac by measurements and MC calculations. They reported a good agreement between different implemented algorithms in Eclipse TPS with MC results and measurements that indicated significant increased dose for 10 × 10 cm² field size. This result is consistent with our data. For a field size of 4 × 4 cm² the maximum differences up to 33% were found for TPS calculations and measurement. From our data the maximum decreased dose of 19% and the related ICF of 1.25 were calculated for 5 × 5 cm² field size. Implementation of algorithms with higher accuracy in TPSs to correct this difference is essential in clinical practices. Ding et al. (2004) ⁽¹⁹⁾ investigated the photon beam models implemented in the CMS FOCUS TPS to predict of absorbed dose in heterogeneous media. The maximum dose difference of 6.9 % in lung analogue was found for the Clarkson algorithm with 5 × 5 cm² field size and 6MV photon beam. They recommended the MGS as the accurate dose calculation algorithm (with difference of 0.3%) when heterogeneous media are in the small treatment fields.

In contrast to the large fields, for the small field sizes such as 2 × 2 cm², the dose decreases rapidly in first depths of lung tissue and then increase significantly beyond the lung region compared to the homogeneous soft tissue. The maximum dose reduction in lung region was 19.5% and 4.2 % for lung density of 0.25 and 0.5gr/cm³, respectively. Mesbahi *et al.* (2014) ⁽⁶⁾ reported a dose reduction of 13% for field size of 2 × 2 cm². In another study, Stathakis *et al.* (2012) ⁽²⁰⁾ calculated the dose reduction in presence of 5 cm lung thickness for 6 MV photon and the maximum dose reduction in lung was reported approximately 16% for 2 × 2 cm² field size. The ICF for underestimated dose region in lung tissue with density of 0.25 and 0.5gr/cm³

was extended to 0.84 and 0.95 for 2 × 2 cm² field size, respectively. This dose reduction has been reported in several studies and is more pronounced for smaller field sizes, lower lung densities and higher photon energies. Lower scattered photons and lateral electronic disequilibrium in these situations cause significant reduction in lung dose. As presented in figure 3.a and 4.a the lateral electronic disequilibrium effect is important for small fields especially for the low density tissues. The electrons produced from Compton interaction can transfer its energy to region outside the applied field where the Compton electron range is greater than the distance of interaction point within a field to the field edge. This lateral disequilibrium is more complicated for low density medium such as lung tissue compared to soft tissue due to the wider range of these electrons. Hence, reduction of absorbed dose within the used field is more crucial for low density mediums. From literatures, more algorithms implemented in different TPSs are failed to accurately estimate absorbed dose in lung tissue due to this significant lateral disequilibrium ^(4, 6, 19-22). Furthermore, lateral disequilibrium would be more significant followed to use of higher photon energy. Increase photon energy increases the energy and range of Compton electron and, consequently, more energy can transfer to the outside of field. Kim YL *et al.* (2016) confirmed that Dose calculation algorithms play a very important role in predicting the explicit dose distribution; instantly, the PDD of air density slab for the Acuros XB (AXB) algorithm was differed by an average of 20% in comparison with other algorithms ⁽²³⁾. da Rosa *et al.* (2010) using the thermoluminescent dosimetry measured more increased and decreased doses compared to our calculated data for 10 × 10 and 2 × 2 cm² field sizes, respectively ⁽²²⁾. These discrepancies are expected due to apply the higher energy of 15 MV photon beam. In all our studied cases, dose was increased at the behind depths of lung tissue where non-targeted health tissues are located and need to be protected due to the lower attenuation of primary photon in passing of the lung tissue. Accurately knowing

the magnitude of these increased doses and apply the related ICFs is important to establish an optimal treatment planning in thorax irradiation. Implementation of these ICFs in TPSs or considering them in manual calculations to determine the actual delivered dose to the target is curial and recommended.

CONCLUSION

Presence of lung tissue in irradiation field perturbs the dose distribution and the magnitude of these decreased or increased doses is highly depended to the lung density and field size. Our MC model and the estimated ICFs could be useful to accurately calculate the dose distribution in radiotherapy of lung tumours.

ACKNOWLEDGEMENTS

This study was a part of MSc thesis of Zohal Ghahremani and supported financially by the research affairs of Ahvaz Jundishapur University of Medical Sciences, Ahvaz, Iran (Grant number: U-95089).

Ethical approval

This research does not contain any study with human participants or animals performed by any of the authors. The other ethical issues have been taken into account.

Conflicts of interest: Declared none.

REFERENCES

1. American Cancer Society. Cancer Facts & Figures 2008. Atlanta: American Cancer Society.
2. Allisy-Roberts P, Ambrosi P, Bartlett DT, Coursey BM, DeWerd LA, Fantuzzi E, et al. (2006) Report 76: Measurement quality assurance for ionizing radiation dosimetry. *Journal of the International Commission on Radiation Units and Measurements*, **6(2)**: NP-NP.
3. Glide-Hurst CK and Chetty IJ (2014) Improving radiotherapy planning, delivery accuracy, and normal tissue sparing

- using cutting edge technologies. *J Thorac Dis*, **6(4)**: 303-318.
4. Tissue inhomogeneity corrections for MV photon beams Report of Task Group No. 65 of the Radiation Therapy Committee of the American Association of Physicists in Medicine. Madison: Medical Physics Publishing; 2004. American Association of Physicists in Medicine (AAPM) Report 85.
5. Keall PJ, Kini VR, Vedam SS, Mohan R (2002) Potential radiotherapy improvements with respiratory gating. *Australas Phys Eng Sci Med*, **25(1)**: 1-6.
6. Mesbahi A, Dadgar H, Ghareh-Aghaji N, Mohammadzadeh M (2014) A Monte Carlo approach to lung dose calculation in small fields used in intensity modulated radiation therapy and stereotactic body radiation therapy. *J Cancer Res Ther*, **10(4)**: 896-902.
7. Giraud P, Garcia R (2010) Respiratory gating for radiotherapy: main technical aspects and clinical benefits. *Bull Cancer*, **97(7)**: 847-856.
8. Chang-li R, Yu-xin C, Lu-zhou W, WU-bing, Qi-bin S (2015) The influence of respiratory motion on dose distribution of 3D-CRT and IMRT- A simulation study. *Int J Radiat Res*, **13(1)**: 39-43.
9. Altunbas C, Kavanagh B, Dzingale W, Stuhr K, Gaspar L, Miften M (2013) Dosimetric errors during treatment of centrally located lung tumors with stereotactic body radiation therapy: Monte Carlo evaluation of tissue inhomogeneity corrections. *Med Dosim*, **38(4)**: 436-41.
10. Senthilkumar S, Ramakrishnan V (2011) Fabrication of low cost in-house slab homogeneous and heterogeneous phantoms for lung radiation treatment. *Int J Radiat Res*, **9(2)**: 109-19.
11. Sterpin E, Salvat F, Olivera G, Vynckier S (2009) Monte Carlo evaluation of the convolution/superposition algorithm of Hi-Art tomotherapy in heterogeneous phantoms and clinical cases. *Med Phys*, **36(5)**: 1566-1575.
12. Andreo P, Burns DT, Huq MS, Kanai T, Iaitano F, Symth VG, et al. (2000) IAEA; TRS-398: Absorbed dose determination in external beam radiotherapy: An International code of practice for dosimetry based on standards of absorbed dose to water. Vienna: IAEA: *International atomic energy agency*, **10**: 46-80.
13. Rogers DW, Faddegon BA, Ding GX, Ma CM, We J, Mackie TR (1995) BEAM: a Monte Carlo code to simulate radiotherapy treatment units. *Med phys*, **22(5)**: 503-524.
14. White DR, Booz J, Griffith RV, Spokas JJ, Wilson IJ (1989) Report 44. *Journal of the International Commission on Radiation Units and Measurements*, **23(1)**: NP-NP.
15. Fraser D, Parker W, Seuntjens J (2009) Characterization of cylindrical ionization chambers for patient specific IMRT QA. *J Appl Clin Med Phys*, **10(4)**: 2923.
16. Chung H, Jin H, Dempsey JF, Liu C, Palta J, Suh TS, et al. (2005) Evaluation of surface and build-up region dose for intensity-modulated radiation therapy in head and neck cancer. *Med phys*, **32(8)**: 2682-2689.
17. Venselaar J, Welleweerd H, Mijneer B (2001) Tolerances for the accuracy of photon beam dose calculations of treatment planning systems. *Radiother Oncol*, **60(2)**: 191-

- 201.
18. Mesbahi A, Thwaites DI, Reilly JA (2006) Experimental and Monte Carlo evaluation of Eclipse treatment planning system for lung dose calculations. *Rep Pract Oncol Radiother*, **11(3)**: 123-133.
19. Ding W, Johnston PN, Wong TP, Bubb IF (2004) Investigation of photon beam models in heterogeneous media of modern radiotherapy. *Australas Phys Eng Sci Med*, **27(2)**: 39-48.
20. Stathakis S, Esquivel C, Quino LS, Myers P, Calvo O, P M (2012) Accuracy of the small field dosimetry using the acuros XB dose calculation algorithm within and beyond heterogeneous media for 6 MV photon beams. *Int J Med Phys Clin Eng Radiat Oncol*, **1**: 78-87.
21. Asnaashari K, Nodehi MR, Mahdavi SR, Gholami S, Khosravi HR (2013) Dosimetric comparison of different inhomogeneity correction algorithms for external photon beam dose calculations. *J Med Phys*, **38(2)**: 74-81.
22. da Rosa LA, Cardoso SC, Campos LT, Alves VG, Batista DV, Facure A (2010) Percentage depth dose evaluation in heterogeneous media using thermoluminescent dosimetry. *J Appl Clin Med Phys*, **11(1)**: 117-127.
23. Kim YL, Suh TS, Choe BY, Choi BO, Chung JB, Lee JW, et al. (2016) Dose distribution evaluation of various dose calculation algorithms in inhomogeneous media. *Int J Radiat Res*, **14(4)**: 269-78.